Volume 9, Number 5
1009-1963/2000/09(05)/0359-09
CHINESE PHYSICS
May, 2000
© 2000 Chin. Phys. Soc.

DIFFUSION PARAMETERS DEPENDENT OSCILLATION CHARACTERISTICS IN Ti-DIFFUSED Nd:$LiNbO_3$ CHANNEL WAVEGUIDE LASER*

Zhang De-long(张德龙), Chen Cai-he(陈才和), and Ding Gui-lan(丁桂兰)
Department of Opto-Electronics Information Engineering, College of Precision Instrument and Opto-Electronics Engineering, Tianjin University, Tianjin 300072, China;
State Key Laboratory of Opto-Electronic Information Science and Technology, Ministry of Education, Tianjin 300072, China

(Received 28 August 1999)

The TM mode size, effective refractive index, effective pump area and coupling efficiency between pump and laser modes as function of Ti-stripe initial width W, diffusion temperature T and Ti-stripe initial thickness H in c-cut Ti-diffused Nd:$LiNbO_3$ waveguide laser have been theoretically investigated using variational method. The main features of the mode sizes in terms of these diffusion parameters were collected and compared with the published experimental results, a qualitative agreement has been obtained. The effective pump area, being proportional to threshold pump power, reveals weak dependences on both W and H in the considered respective ranges 4–16 μm and 40–160 nm, and a strong dependence on T(950–1100 ℃); while the coupling efficiency relative to slope efficiency hardly changes (with values 0.82–0.85) with these parameters.

PACC: 4255R; 4260H; 4280L; 4282

I. INTRODUCTION

The functionality of waveguide and bulk $LiNbO_3$ optical devices has increased dramatically over the past few years. Recent advances in the technologies of rare-earth doping in this material have demonstrated the potential for commercially attractive lasers and nonlinear optical sources which are compact, efficient, inexpensive and manufacturable. These devices could find use in a wide range of applications including telecommunications, range finding, military counter measures, optical data storage and remote sensing. Nd-doped $LiNbO_3$ is a promising solid laser material that combines the good laser characteristics of Nd^{3+} with the electro-optic, acousto-optic and nonlinear optical properties of $LiNbO_3$. Consequently, continuous wave (CW) operation annealed proton exchange (APE), titanium diffusion (TD) Nd:MgO:$LiNbO_3$, TD Nd:$LiNbO_3$ channel waveguide lasers[1−7] and integrated devices including FM mode-locked[8], Q-switched[9] and pulsed[10] waveguide lasers have been successfully demonstrated in recent years. Figs.1(a) and 1(b) illustrate the geometry of Ti-stripe before diffusion and the schematic structure of the fabricated Ti-diffused Nd-doped $LiNbO_3$ channel waveguide.

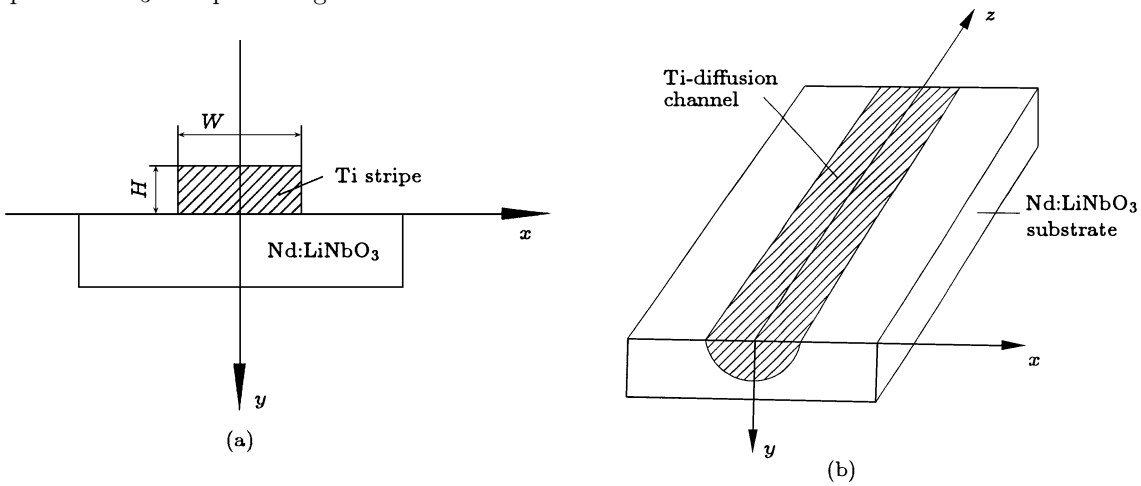


Fig.1. (a) Geometry of Ti-stripe used to fabricate a Nd:$LiNbO_3$ channel waveguide, (b) Ti-diffused Nd-doped $LiNbO_3$ channel waveguide.x and y are the coordinates in the plane perpendicular to the waveguide axis, which is parallel to the propagation direction z. Crystallographic axis c coincides with the direction of y axis.

* Project supported by 21st Century Youth Natural Science Foundation of Tianjin, China (Grant No. 963700911).

Several papers have been concerned with laser oscillation theory. By assuming Gaussian/two-half-Gaussian and Gaussian/Hermite-Gaussian mode field distributions in the direction of width/depth in APE and TD waveguides, respectively, Lallier *et al.*[4] and Brinkmann *et al.*[5] evaluated the threshold pump power and slope efficiency using the expressions derived by Digonnet and Geata[11] and compared with their measured results. Lee and Sheu[12] proposed a pure theoretical analysis for the Ti-diffused Nd:MgO:$LiNbO_3$ waveguide lasers with nonuniform concentration distribution by using the evolution equations of the pumping light and amplified spontaneous emission (ASE), and by varying some characteristic parameters such as the launched pump power, the length of the waveguide, the reflectance of the waveguide endface and waveguide loss, etc., the laser output, pump and laser evolutions have been evaluated and discussed.

The optimization of the laser efficiency of integrated optical devices requires not only the knowledge mentioned above, but also the knowledge of dependence of some physical quantities (e.g. mode size, effective refractive index, threshold pump power and slope efficiency, etc.) on waveguide fabrication parameters. These studies may improve the understanding of the physical phenomena involved and offer a guidance to design more efficient laser devices. However, information about this has not been reported so far. In this work, we report the theoretical results of Ti-diffused Nd:$LiNbO_3$ waveguide laser in this aspect. By assuming Gaussian/Hermite-Gaussian mode field distributions in the direction of width/depth in the Ti-diffused waveguide and using variational technique, the TM laser (λ_s=1085 nm), pump (λ_p=815 nm) mode sizes and effective refractive index against the controllable waveguide fabrication parameters (i.e., initial Ti-stripe width, diffusion temperature and initial Ti-stripe thickness) are numerically calculated, and then, the corresponding effective pump area and coupling efficiency between pump and laser modes, which are proportional to the threshold pump power and slope efficiency, respectively, are computed.

Ⅱ. CALCULATION METHOD

A. Variational analysis

The variational analysis of Ti:$LiNbO_3$ waveguides provides an effective approach in determining simultaneously the mode sizes and the propagation constant (the effective refractive index)[13], which are very useful in optimizing and designing waveguide devices. This method has the advantages of speediness, simplicity and high accuracy.

According to Strake *et al.*[14], for TM modes guided in a *c*-cut Ti-diffused $LiNbO_3$ waveguide, the scalar, two dimensional wave equation for the dominant field component $\phi(x,y)$ can be expressed as:

$$\left[\frac{\partial^2}{\partial x^2}+\left(\frac{n_{\mathrm{e}}(x,y)}{n_{\mathrm{o}}(x,y)}\right)^2\frac{\partial^2}{\partial y^2}\right]\phi(x,y) + k_0^2 n_{\mathrm{e}}^2(x,y)\phi(x,y)=\beta^2\phi(x,y), \tag{1}$$

in which k_0 is the wavenumber in free space, $\beta = k_0 N_{\mathrm{eff}}$ is the guided mode propagation constant, N_{eff} is the effective refractive index. $n_{\mathrm{e}}(x,y)$ and $n_{\mathrm{o}}(x,y)$ are the extraordinary and ordinary refractive index profiles, respectively. According to Hocker and Burns[15], for a *c*-cut Ti:$LiNbO_3$ channel waveguide with the initial Ti-stripe width W they can be expressed as:

$$n_{\mathrm{e,o}}^2(x,y)=\begin{cases}1 & y<0\\ n_{\mathrm{eb},ob}^2+(n_{\mathrm{es},os}^2-n_{\mathrm{eb},ob}^2)f\left(\dfrac{y}{d_{y_{\mathrm{e,o}}}}\right)g\left(\dfrac{2x}{W}\right) & y>0,\end{cases} \tag{2}$$

where

$$f\left(\frac{y}{d_{y_{\mathrm{e,o}}}}\right)=\exp\left(\frac{y^2}{d_{y_{\mathrm{e,o}}}^2}\right) \tag{3}$$

and

$$g\left(\frac{2x}{W}\right)=\frac{1}{2}\left[\mathrm{erf}\left(\frac{W}{2d_{x_{\mathrm{e,o}}}}\left(1+\frac{2x}{W}\right)\right)+\mathrm{erf}\left(\frac{W}{2d_{x_{\mathrm{e,0}}}}\left(1-\frac{2x}{W}\right)\right)\right], \tag{4}$$

here d_x and d_y are diffusion width and depth, respectively, which can be computed by:

$$d_x=2\sqrt{D_x t} \tag{5}$$

and

$$d_y=2\sqrt{D_y t}, \tag{6}$$

where t is the diffusion time, D_x and D_y are the dif-

fusion coefficients given by the following expressions:

$$D_x = D_0^x \exp\left(-\frac{E_0^x}{KT}\right), \tag{7}$$

$$D_y = D_0^y \exp\left(-\frac{E_0^y}{KT}\right), \tag{8}$$

where D_0^x, D_0^y are the diffusion constants and E_0^x, E_0^y are the activation energies in the x and y direction, respectively. Numerical data of these parameters can be found in literature.[16]

In Eq.(2) n_b is the refractive index of $LiNbO_3$, n_s is the surface index of the waveguide and it is given by the equation:

$$n_{es,os} = n_{eb,ob} + \Delta n_{e,o}, \tag{9}$$

in which $n_{eb,ob}$ can be obtained by a generalized Sellmeier equation[17], and $\Delta n_{e,o}$ are calculated by[16]:

$$\Delta n_{e,o} = \left(B_0(\lambda) + B_1(\lambda)\frac{H}{d_{y_{e,o}}}\right)\left(\frac{H}{d_{y_{e,o}}}\right)^{\alpha_{e,o}}, \tag{10}$$

where for the ordinary ray:

$$B_0(\lambda) = 0.0653 - 0.0315\lambda + 0.00709\lambda^2,$$
$$B_1(\lambda) = 0.478 + 0.464\lambda - 0.348\lambda^2;$$

and for the extraordinary ray:

$$B_0(\lambda) = 0.385 - 0.43\lambda + 0.171\lambda^2,$$
$$B_1(\lambda) = 9.13 + 3.85\lambda - 2.49\lambda^2.$$

In Eq.(10) H is the initial thickness of Ti stripe and the fitted constants $\alpha_e = 0.83$, $\alpha_o = 0.53$.

To simplify Eq.(1), in Fig.2 we show surface plots of the ratio of $(n_e(x,y)/n_o(x,y))^2/(n_e/n_o)^2$ at wavelengths 1085 and 815 nm (for a waveguide fabricated by indiffusing 6 μm width, 100 nm thickness Ti-stripe at 1050 ℃ during 8.3333 h). One can see that $(n_e(x,y)/n_o(x,y))^2/(n_e/n_o)^2 \approx 1$, i.e., $(n_e(x,y)/n_o(x,y))^2 \approx (n_e/n_o)^2$, consequently, Eq.(1) can be simplified as:

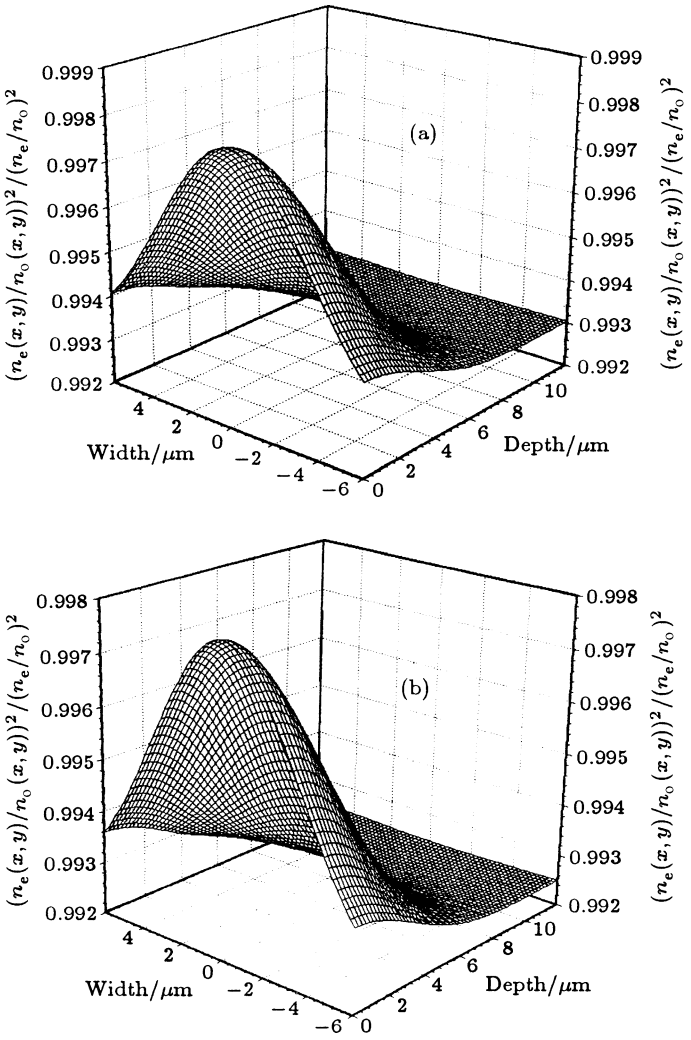


Fig.2. Surface plots of the ratio $(n_e(x,y)/n_o(x,y))^2/(n_e/n_o)^2$ for (a) 1085 nm, (b) 815 nm.

$$\left[\frac{\partial^2}{\partial x^2}+\left(\frac{n_{\rm e}}{n_{\rm o}}\right)^2\frac{\partial^2}{\partial y^2}\right]\phi(x,y)+k_0^2n_{\rm e}^2(x,y)\phi(x,y)=\beta^2\phi(x,y). \tag{11}$$

Then, the propagation constant β can be obtained from the variational equation:

$$\beta^2=\frac{\iint\phi(x,y)\left(\frac{\partial^2}{\partial x^2}+\left(\frac{n_{\rm e}}{n_{\rm o}}\right)^2\frac{\partial^2}{\partial y^2}\right)\phi(x,y){\rm d}x{\rm d}y+k_0^2\iint n_{\rm e}^2(x,y)\phi^2(x,y){\rm d}x{\rm d}y}{\iint\phi^2(x,y){\rm d}x{\rm d}y}, \tag{12}$$

here $\phi(x,y)$ is the fundamental transverse field distribution of TM mode under consideration. According to Marcuse[18], it is well described by symmetric Gaussian function in the direction of width and by Hermite-Gaussian trial solution in the direction of depth. As a result, the normalized mode field distribution can be written as:

$$\phi(x,y)=\frac{4y}{\sqrt{\pi W_xW_y^3}}\exp\left[-\left(\frac{x^2}{W_x^2}+\frac{y^2}{W_y^2}\right)\right], \tag{13}$$

where W_x and W_y are the mode sizes.

Substituting Eqs.(2) and (13) into (12), we have

$$\begin{aligned}\beta^2=&k_0^2n_b^2+\frac{4(n_s^2-n_b^2)k_0^2}{\sqrt{2\pi}W_x}\left(1+\frac{W_y^2}{2d_y^2}\right)^{-3/2}Q\\&-\frac{1}{W_x^2}-\left(\frac{n_{\rm e}}{n_{\rm o}}\right)^2\frac{3}{W_y^2},\end{aligned} \tag{14}$$

where

$$Q=\int_0^{+\infty}g\left(\frac{2x}{W}\right)\exp\left(-\frac{2x^2}{W_x^2}\right){\rm d}x. \tag{15}$$

One can see from Eq.(14) that the propagation constant, i.e., the effective refractive index, for a given wavelength, is determined mainly by the difference between two competing terms, one term depends on the overlap of the mode intensity distribution with the index profile (i.e., the second term in Eq.(14)), and the other term depends inversely on the square of the mode size (the last two terms in Eq.(14)). Inserting the above known values of λ, W, n_b, n_s, d_x and d_y into Eq.(14), the optimum values of W_x and W_y yield the largest value of β^2, namely β_m^2, then, the corresponding effective refractive index can be readily obtained.

B. Laser oscillation characteristics

Starting with rate equation of a four level system and taking into account the spatial distributions of pump and laser mode, Kubodera and Otsuka[19] have derived general expressions of threshold pump power and slope efficiency for a coaxially pumped waveguide laser, and they can be rewritten as

$$P_{\rm th}=\frac{h\nu_{\rm p}}{\eta_{\rm a}\sigma\tau_{\rm f}}\frac{\delta_1}{2}A_{\rm eff}, \tag{16}$$

and

$$S_e=\frac{T_2}{\delta_1}\frac{\lambda_p}{\lambda_s}\eta_{\rm a}\eta_{\rm c}, \tag{17}$$

where δ_1 is the round-trip cavity loss, $h\nu_{\rm p}$ is the pump photon energy, $\eta_{\rm a}$ is the waveguide absorption efficiency for pump light, σ is the stimulated emission cross section of Nd^{3+}, $\tau_{\rm f}$ is the fluorescence lifetime. $A_{\rm eff}$ is the effective pump area and is given by

$$A_{\rm eff}=\left(l\int_{\rm cavity}s_{01}(x,y,z)r_0(x,y,z,){\rm d}x{\rm d}y{\rm d}z\right)^{-1}, \tag{18}$$

where l is the cavity length, $s_{01}(x,y,z)$ and $r_0(x,y,z)$ are the normalized laser and pump mode intensity distributions, respectively, and are expressed as the square of $\phi(x,y)$.

In Eq.(17), T_2 is the transmittance of the output mirror at laser wavelength, λ_p/λ_s is the ratio of pump-to-laser wavelength. $\eta_{\rm c}$ is the coupling efficiency between laser mode and pump mode and it can be expressed as

$$\eta_{\rm c}=\frac{I_1^2}{I_2}, \tag{19}$$

where

$$I_1=\int_{\rm cavity}s_{01}(x,y,z)r_0(x,y,z){\rm d}x{\rm d}y{\rm d}z \tag{20}$$

and

$$I_2=\int_{\rm cavity}s_{01}^2(x,y,z)r_0(x,y,z){\rm d}x{\rm d}y{\rm d}z. \tag{21}$$

Ignoring the z-dependent variations, substituting $s_{01}(x,y,z)$ and $r_0(x,y,z)$ into Eqs.(18)–(21), one can obtain

$$A_{\rm eff}=\frac{\pi}{12}\frac{\sqrt{(W_{xs}^2+W_{xp}^2)(W_{ys}^2+W_{yp}^2)^5}}{W_{ys}^2W_{yp}^2} \tag{22}$$

and

$$\eta_{\rm c} = \frac{3}{5}\frac{W_{xs}W_{ys}^3\sqrt{(W_{xs}^2+2W_{xp}^2)(W_{ys}^2+2W_{yp}^2)^7}}{(W_{xs}^2+W_{xp}^2)(W_{ys}^2+W_{yp}^2)^5}. \tag{23}$$

In the above two expressions, W_{is} and $W_{ip}(i = x, y)$ represent the laser and pump mode sizes, respectively. Inserting their values calculated by the variational method, one can obtain the corresponding values of $A_{\rm eff}$ and $\eta_{\rm c}$.

One can see from Eqs.(16) and (17) that factors influencing the laser efficiency are laser material properties $(\sigma, \tau_{\rm f})$, pump photon energy $(h\nu_{\rm p})$, absorption efficiency for the pump light $(\eta_{\rm a})$, output coupler loss (T_2), ratio of pump-to-laser wavelength (λ_p/λ_s), round-trip cavity loss (δ_1), stimulated emission cross section of $Nd^{3+}(\sigma)$, effective pump area $(A_{\rm eff})$ and coupling efficiency between pump mode and laser mode $(\eta_{\rm c})$. Of these the last four are closely relative to the waveguide fabrication parameters. The waveguide fabrication parameters dependent Nd^{3+} stimulated emission cross section has been proposed by Lallier *et al.* for x-cut APE Nd:MgO:$LiNbO_3$ waveguide laser[4]; and the optical losses of Ti:$LiNbO_3$ vs diffusion temperature were investigated at the wavelength 1.15 μm by Fukuma and Noda.[20] In the following we establish the variations of effective pump area and coupling efficiency with these parameters. We limit our discussion to a c-cut Ti-diffused Nd:$LiNbO_3$ waveguide laser and the calculations are performed for fundamental TM mode at both laser wavelength 1085 nm and pump wavelength 815 nm.

Ⅲ. CALCULATED RESULTS AND DISCUSSIONS

A. Mode sizes and effective refractive index

A C program was written to compute the mode sizes W_x and W_y using Eq.(14). The calculation accuracy is 10^{-6}. The variations of mode sizes W_{is} and W_{ip} with the diffusion parameters are plotted in Fig.3. Fig.3(a) shows the variations of mode sizes with the stripe width W for the waveguide fabricated by indiffusing 100 nm thick Ti-stripe at 1050 ℃ during 8.3333 h; Fig.3(b) is for the case of diffusion temperature T for the guide formed by indiffusing 6 μm wide, 100 nm thick Ti-stripe during 8.3333 h; and Fig.3(c) gives the curves of mode sizes versus initial Ti-stripe thickness H for the waveguide achieved by indiffusing 6 μm width Ti-stripe in the rate 12 nm/h at 1050 ℃.

From these plots one can find that the plot of each pair of W_x and W_y can be made to coincide approximately by translating the upper s-curve downward from the laser wavelength to the pump wavelength. This implies that the mode sizes increase with a rise in wavelength. Furthermore, for any one of the two wavelengths considered, there is an intersection for the pair of W_x and W_y, where $W_x = W_y$. We refer to it as the iso-mode-size intersection (IMSI). Moreover, for any one of the diffusion parameters, these intersections locate nearly in the same position. It can be seen from Fig.3(a), that this position is near the width $W = 5.8\,\mu$m; for $W < 5.8\,\mu$m, $W_x < W_y$ and both decrease with increasing W; when $W > 5.8\,\mu$m, however, $W_x > W_y$, W_x decreases further and passes through a minimum, increases slowly and then quickly, as a result of weaker optical confinement in the direction of width; while W_y decreases continueously, then tends gradually to a constant, indicating that W_y does not change with increasing W when the optical confinement in the direction of width is weak enough. In Fig.3(b) the ISMI's are approximately located at about 1050 ℃. Both W_x and W_y show remarkable increase with increasing diffusion temperature T and this is supported by the near-field mode observed by Fukuma and Noda at the wavelength 1.15 μm.[20] For T <1050 ℃, $W_x > W_y$, for T >1050 ℃, $W_x < W_y$. The dependence of mode size on the initial Ti-stripe thickness H in the studied range 40–160 nm is found to be weaker than on the other two parameters, as shown in Fig.3(c). The IMSI's appear near 100 nm.

The mode sizes as a function of W (in the range of 5–10 μm), H (in the region of 70–110 nm) have been measured at 1.32 μm wavelength by Korotky *et al.*[13], who defined the mode sizes as the full width at half maximum (FWHM). Here we cannot give an accurate comparison with the measured data due to the differences in wavelengths and diffusion conditions, but making a comparison of the general behavior is possible. The general tendencies of our plots are in agreement with the measured ones for the diffusion parameters W and H in the concerned ranges as shown in Fig.1 and Fig.2 of Ref.[13]. These tendencies include the decrease of the mode size with W or H and $W_x > W_y$. They also calculated the dependence of mode size on the two parameters using variational technique. The main difference with this model is the employing of the refractive index profiles. They first calculated normalized mode sizes versus W which, however, did not compare with the experimental data; then, geometrical mean mode size and mode size ratio

and, consequently, the former can well cover their experimental data, whereas the latter overpredicts the measured values by nearly 20 percent.

The plots of the corresponding effective refractive index N_{eff} for both considered wavelengths are shown in Fig.4. To facilitate the discussion, the surface refractive index n_{es} versus $T(H)$ is also given in Figs.4(b), (4c) (n_{es} is independent of W and is held constant with the values of 2.165237 for 1085 nm and 2.186046 for 815 nm). The plots of Fig.4 reveal two features: one is similar as observed in Fig.3, i.e., the curve can be approximately translated upward from laser wavelength to pump wavelength, and the other is that the values of N_{eff}, for a given wavelength, are larger than that of n_{eb} (2.152452 for 1085 nm and 2.171969 for 815 nm, calculated from Sellmeier equation[17] under assumption of the composition of Li_2O 48.5% and at ambient temperature 24.5 ℃) and smaller than that of n_{es}. This is consistent with the guided wave theory. In addition, N_{eff} increases steadily with a rise in stripe width W and thickness H as shown in Figs.4(a) and 4(c), and the former tends gradually to saturation when W is large enough. And, as shown in Fig.4(b), N_{eff} decreases as the diffusion temperature T is increased.

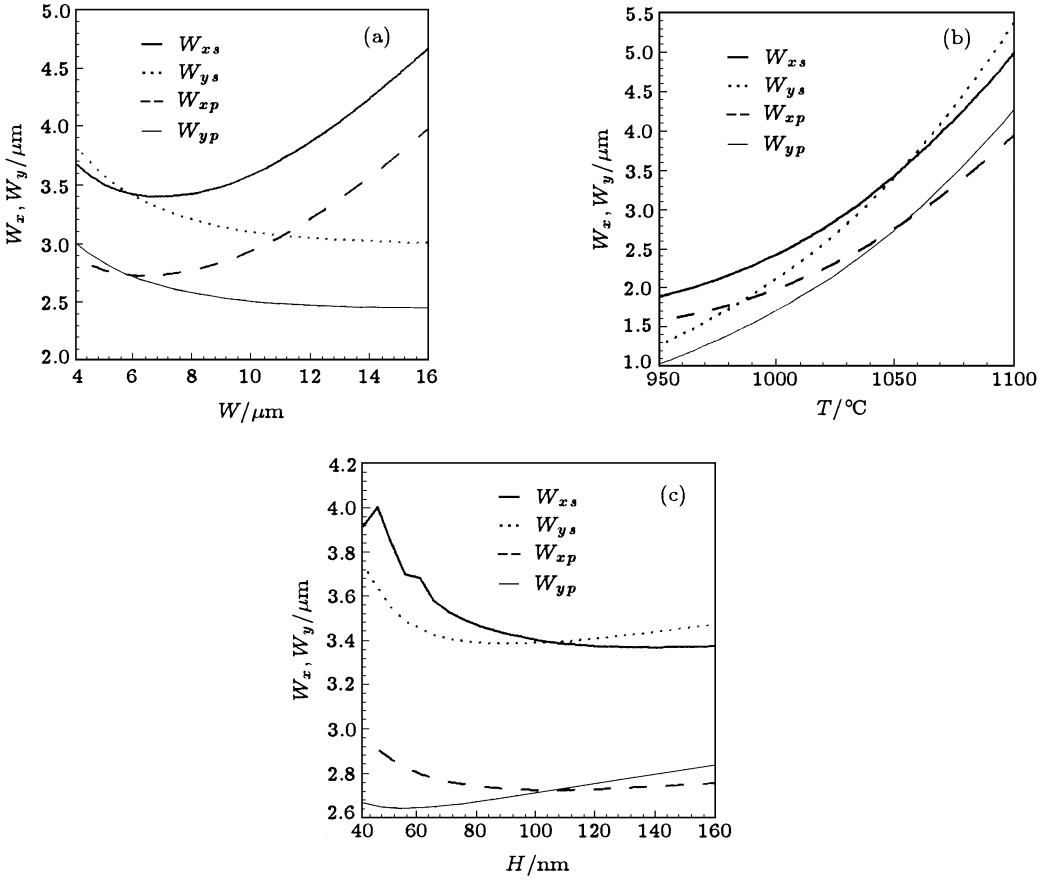


Fig.3. (a) Waveguide stripe width W, (b) diffusion temperature T and (c) initial Ti-stripe thickness H dependence of laser and pump mode sizes.

B. Effective pump area A_{eff}

From Figs.3(a)–3(c), the effective pump area A_{eff} can be readily calculated by using Eq.(22) and the results are shown in Figs.5(a)–5(c). It is evident that A_{eff} has a weak dependence on both W and H in the considered respective ranges 4–16 μm and 40–160 nm, and a strong dependence on T. In Fig.5(a), A_{eff} has a minimum of 19.68 μm^2 at W =8.5 μm; for W <8.5 μm, A_{eff} decreases with increasing W, and for W >8.5 μm, A_{eff} increases as W is increased further. Nevertheless, the largest difference in the studied range 4–16 μm is merely about 6 μm^2, that is approximately three times lower than the minimum value 19.68 μm^2, indicating that the Ti-stripe width cannot influence significantly on the threshold pump power via A_{eff}. In Fig.5(b), A_{eff} increases strongly with the increase of diffusion

temperature T. Its values at 1100 ℃ is 47.44 μm^2, that is nearly eleven times higher than the figure 4.38 μm^2 at 950 ℃, showing that the diffusion temperature strongly influences on the threshold pump power via A_{eff}, and the lower the diffusion temperature, the smaller the threshold pump power. It should be noted that the multimode region may be approached as the diffusion temperature is lowered. Further calculation about this is now in progress. Moreover, the lowering of the diffusion temperature also results in the increase of the optical loss.[20] In Fig.5(c), A_{eff} decreases gradually as H is increased from 40 nm and passes through a minimum of 20.82 μm^2 around H = 105 nm, and then increases only slightly. The largest difference in the considered region is only 6 μm^2, that is 3.7 times lower than the value of the minimum 20.82 μm^2. This means that the Ti-stripe thickness also cannot affect obviously the threshold pump power via A_{eff}.

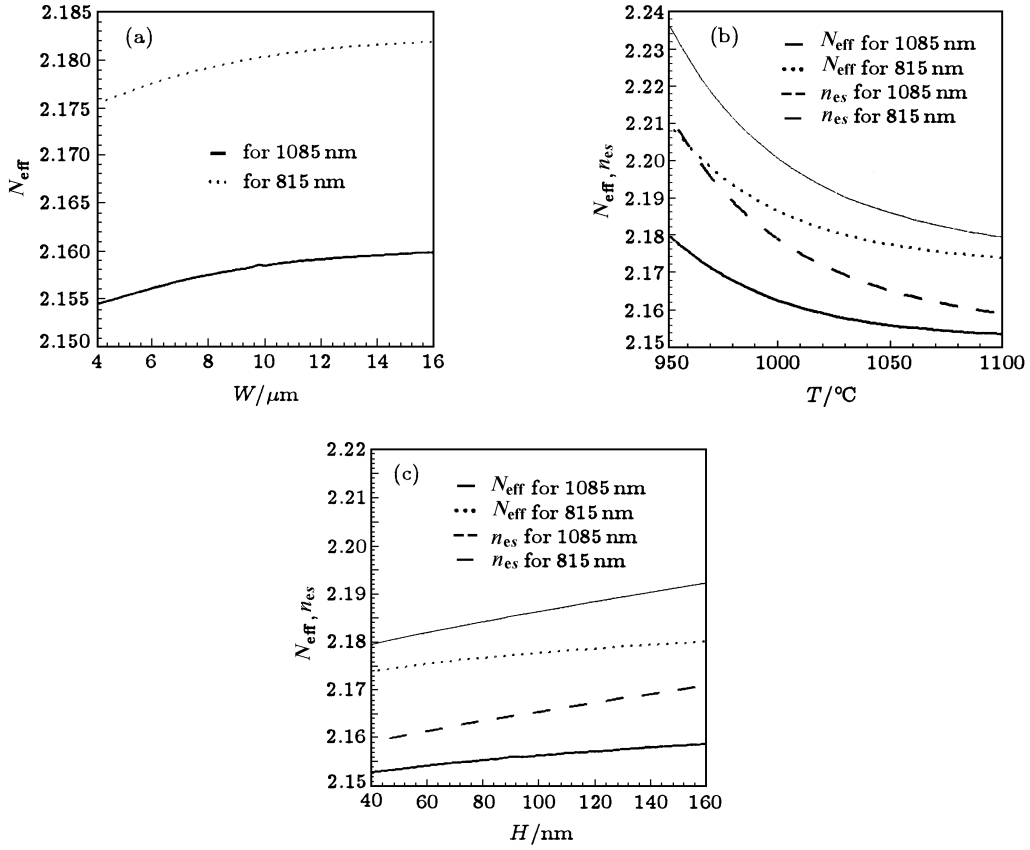


Fig.4. (a) Waveguide stripe width W, (b) diffusion temperature T and (c) initial Ti-stripe thickness (H) dependence of effective refractive index N_{eff}.

C. Coupling efficiency η_c

The plots shown in Figs.6(a), 6(b) and 6(c) are obtained respectively from Figs.3(a), 3(b) and 3(c) on the basis of Eq.(23). We can see from these plots that all curves are nearly straight lines parallel to the abscissas. The values of η_{c} vary only in a very small range of 0.82–0.85, i.e., η_{c} is essentially held constant no matter how these parameters are changed. Hence, we may conclude that high slope efficiency cannot be obtained by optimizing the initial Ti-stripe width, the diffusion temperature and the initial Ti-stripe thickness through the coupling efficiency η_{c}.

To compare the calculated results of A_{eff} and η_{c} with the published experimental data, a calculation is also performed on a c-cut Ti-diffused Nd:MgO:$LiNbO_3$ channel waveguide laser reported by Brinkmann *et al.*[5] In their experiment, the laser action was realized for the waveguide fabricated by indiffusing 6 μm wide, 55 nm thick Ti-stripe at 1060 ℃ during 9 h. These experimental parameters result in the following calculated results: W_{xs} = 5.311 μm, W_{ys} = 5.386 μm, W_{xp} = 3.943 μm and W_{yp} = 4.0242 μm, comparable to the measured data 5.0 ± 0.2, 4.0 ± 0.2, 3.7 ± 0.2 and 2.8 ± 0.2 μm. These theoretical values yield an effective pump area of 50.65 μm^2 and a coupling efficiency of 84.2%. The former, consequently,

leads to a threshold pump power 2.32 mW and is in agreement with the experiment data 2.1 mW, while the latter is in good agreement with the data 83.46%, predicted by using above measured data of mode sizes.

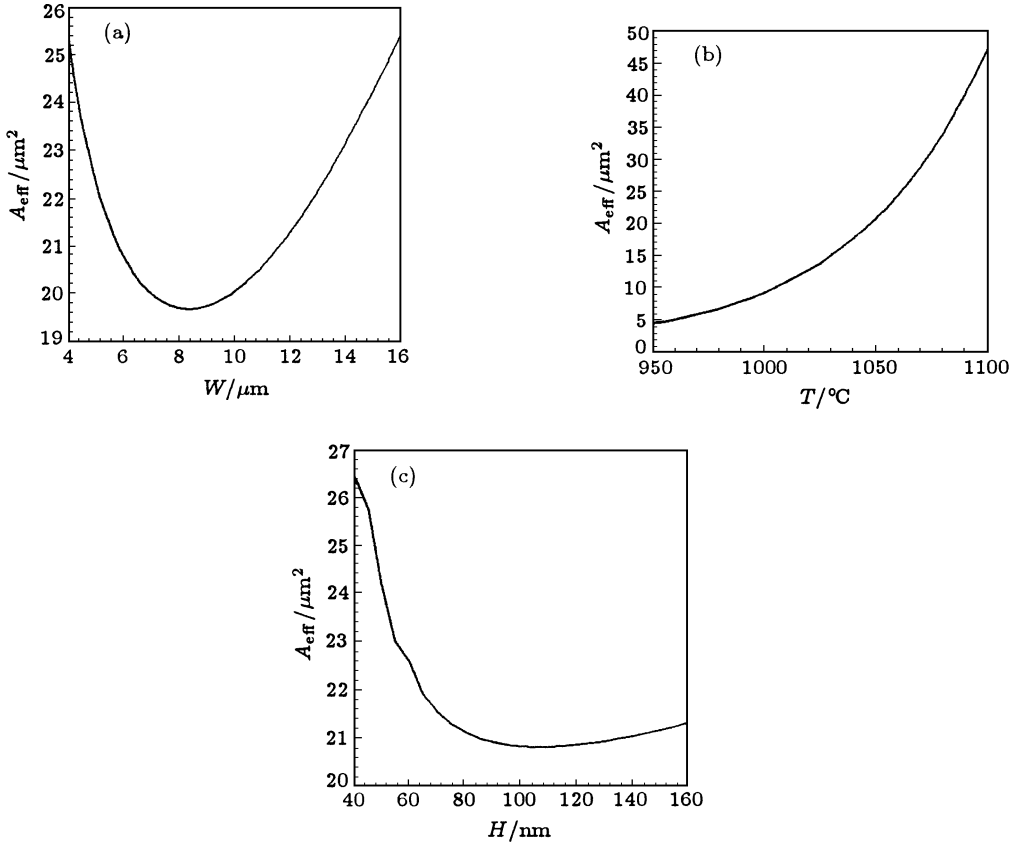


Fig.5. (a) Waveguide stripe width W, (b) diffusion temperature T and (c) initial Ti-stripe thickness H dependence of effective pump area $A_{\rm eff}$.

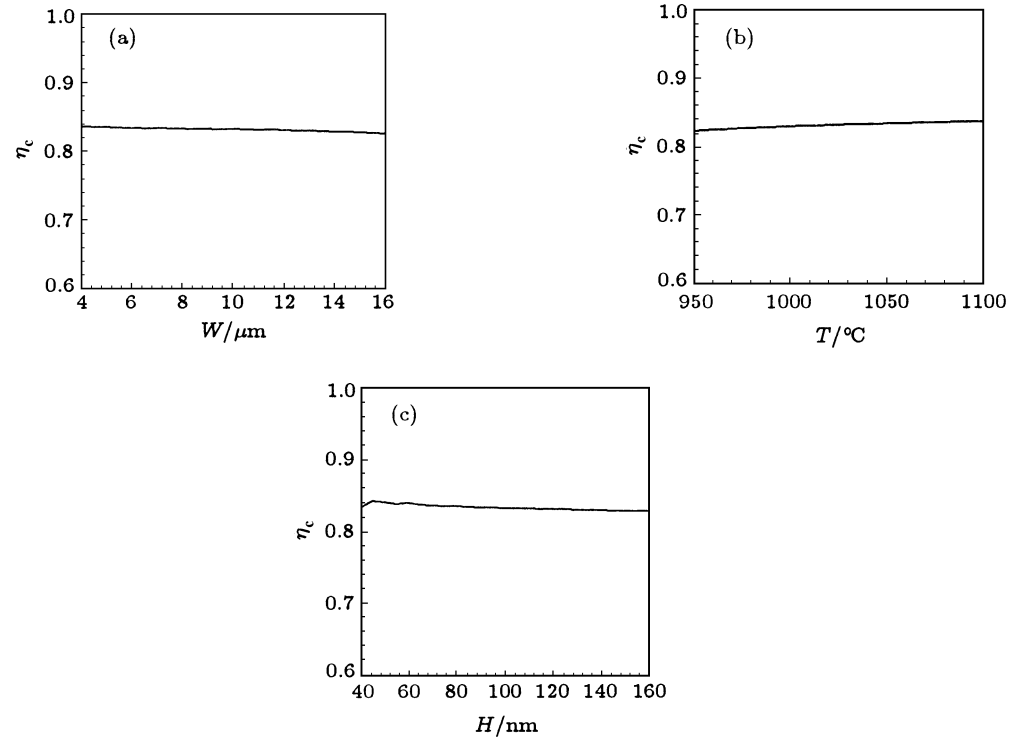


Fig.6. (a) Waveguide stripe width W, (b) diffusion temperature T and (c) initial Ti-stripe thickness H dependence of coupling efficiency η_c.

IV. CONCLUSIONS

The initial Ti-stripe width, thickness and diffusion temperature dependent mode size, effective refractive index, effective pump area and coupling efficiency have been theoretically investigated for c-cut Ti-diffused Nd:$LiNbO_3$ waveguide laser when pumped at wavelength 815 nm. The featurs of mode size against these parameters have been summarized. As compared with the published experimental results, an agreement in general behavior has been obtained. The effective pump area exhibits a weak dependence on the initial Ti-stripe width and thickness, and a strong dependence on the diffusion temperature. The threshold pump power can be effectively lowered by decreasing the diffusion temperature, which, however, results simultaneously in the appearance of the multimodes and the increase of the optical loss of the waveguide. On the other hand, the coupling efficiency is essentially independent of the three parameters, and its value varies in the range of 0.82–0.85, indicating that we cannot obtain high slope efficincy through coupling efficiency, i.e., there are no optimized values of initial Ti-stripe width, diffusion temperature and initial Ti-stripe thickness via coupling efficiency to raise slope efficiency. The preferred selections may be increasing the waveguide absorption efficiency for the pump light and the transmittance of the output mirror and reducing the round-trip cavity loss.

REFERENCES

[1] E. Lallier, J. P. Pocholle, M. Papuchon, C. Grezes-Besset, E. Pelletier, M. De Micheli, M. J. Li, Q. He and D. B. Ostrowsky, *Electron. Lett.*, **25**(1989), 1491.

[2] E. Lallier, J. P. Pocholle, M. Papuchon, M. De Micheli, M. J. Li, Q. He, D. B. Ostrowsky, C. Grezes-Besset and E. Pelletier, *Electron. Lett.*, **26**(1990), 927.

[3] E. Lallier, J. P. Pocholle, M. Papuchon, M. De Micheli, M. J. Li, Q. He, D. B. Ostrowsky, C. Grezes-Besset and E. Pelletier, *Opt. Lett.*, **15**(1990), 682.

[4] E. Lallier, J. P. Pocholle, M. Papuchon, M. De Micheli, M. J. Li, Q. He, D. B. Ostrowsky, C. Grezes-Besset and E. Pelletier, *IEEE J. Quantum Electron.*, **27**(1991), 618.

[5] R. Brinkmann, W. Sohler, H. Suche and C. Wersig, *IEEE J. Quantum Electron.*, **28**(1992), 466.

[6] M. Hempstead, J. S. Wilkinson and L. Reekie, *IEEE Photon. Technol. Lett.*, **4**(1992), 852.

[7] M. Haruna, H. Sewai, H. Nishihara, S. Ikunishi, T. Gozen and H. Tanaka, *Electron. Lett.*, **30**(1994), 412.

[8] E. Lallier, J. P. Pocholle, M. Papuchon, Q. He, M. De Micheli, D. B. Ostrowsky, C. Grezes-Besset and E. Pelletier, *Electron. Lett.*, **27**(1991), 936.

[9] E. Lallier, J. P. Pocholle, M. Papuchon, Q. He, M. De Micheli, and D. B. Ostrowsky, *Electron. Lett.*, **28**(1992), 1428.

[10] E. Lallier, D. Papillon, J. P. Pocholle, M. Papuchon, M. De Micheli, and D. B. Ostrowsky, *Electron. Lett.*, **29**(1993), 175.

[11] M. J. F. Digonnet and C. J. Geata, *Appl. Opt.*, **24**(1985), 333.

[12] C. T. Lee and L. G. Sheu, *J. Lightwave Technology*, **14**(1996), 2268.

[13] S. K. Korotky, W. J. Minford, L. L. Buhl, M. D. Divino and R. C. Alferness, *IEEE J. Quantum Electron.*, **18**(1982), 1796.

[14] E. Strake, G. P. Bava and I. Montrosset, *J. Lightwave Technology*, **6**(1988), 1126.

[15] G. B. Hocker and W. K. Burns, *Appl. Opt.*, **16**(1977), 113.

[16] S. Fouchet, A. Carenco, C. Daguet, R. Guglielmi and L. Riviere, *J. Lightwave Technology*, **5**(1987), 700.

[17] U. Schlarb and K. Betzler, *Ferroelectrics*, **156**(1994), [1983]/99.

[18] D. Marcuse, *IEEE J. Quantum Electron.*, **18**(1982), 393, see also Correction, p.807(1982).

[19] K. Kubodera and K. Otsuka, *J. Appl. Phys.*, **50**(1979), 653.

[20] M. Fukuma and J. Noda, *Appl. Opt.*, **19**(1980), 591.